STUDY OF TITANIUM DIOXIDE NANOTUBES AND NANOPARTICLES FOR ULTRAVIOLET PHOTODETECTION APPLICATION

LOW KAI TI

UNIVERSITI SAINS MALAYSIA

2021

STUDY OF TITANIUM DIOXIDE NANOTUBES AND NANOPARTICLES FOR ULTRAVIOLET PHOTODETECTION APPLICATION

by

LOW KAI TI

Thesis submitted in fulfilment of the requirements
for the degree of
Master of Science

December 2021

ACKNOWLEDGEMENT

First and foremost, I would like to express my deepest gratitude to my supervisor, Assoc. Prof. Dr. Yam Fong Kwong for his invaluable guidance, patience, and endless encouragement to help me achieve outstanding goals in this research work. We had faced many challenges and ups and downs along my research journey. This research study would not have been successful without his heartfelt commitment and guidance.

I would also like to take this golden opportunity to express my greatest appreciation to Dr. Beh Khi Poay for his knowledgeable guidance and informative recommendations for my research work, despite his busy schedule. I have learnt from his considerable practical knowledge and skills, making me a better research student.

A great acknowledgement also goes to technical team from School of Physics and Nano-Optoelectronics Research and Technology (NOR), Universiti Sains Malaysia (USM), Mr. Yushamdan, Mr Abdul Jamil and Mdm. Ee Bee Choo.

Last but not least, I would like to express my heartfelt gratitude to my beloved parents for their unconditional love, infinite patience, and supports over the years. Without their mental and financial support, I would not have been able to complete my study seamlessly and successfully.

TABLE OF CONTENTS

LIST OF TABLES

Page

LIST OF FIGURES

Page

LIST OF SYMBOLS

a	Lattice constant
A	Area
Å	Angstrom
B	Absorption constant
D	Crystallite size
d	Interplanar spacing
e	Charge of electron
E_g	Energy band gap
h	Plank's constant
I	Current
I_{dark}	Dark current
I_{light}	Photocurrent
I_{ph}	Photocurrent
K	Shape factor
n	Diffraction order
n	Electronic transition
°C	Degree Celsius
P	Light intensity
R	Reflectance
R	Responsivity
S	Sensitivity
V	Voltage
β	Full width at half maximum
ε_a	In-plane strain

ε_c	Out-of-plane strain
θ	Bragg's angle
λ	Wavelength
τ_r	Rise time
τ_f	Fall time
ν	Frequency
$\bar{x}$	Mean diameter

LIST OF ABBREVIATIONS

0D	Zero-dimensional
1D	One-dimensional
CB	Conduction band
C-TiO_2	Commercial TiO_2
EDX	Energy-dispersive X-ray spectroscopy
ENIG	Electroless nickel immersion gold
eV	Electron volt
FE-SEM	Field emission scanning electron microscope
FR-4	Flame retardant-4
FTO	Fluorine-doped tin oxide
FWHM	Full width half maximum
IPA	Isopropryl alcohol
I-t	Current-time
I-V	Current-voltage
LED	Light emitting diode
MONPs	Metal oxides nanoparticles
N/A	No data available
NsM	Nanostructured material
NPs	Nanoparticles
PCB	Printed circuit board
PET	Polyethene terephthalate
PVA	Polyvinyl alcohol
RF	Radiofrequency
SG-TiO_2	Sol-gel derived TiO_2

SMU	Source measuring unit
TNPs	TiO_2 nanoparticles
TNTs	TiO_2 nanotubes
UV	Ultraviolet
VB	Valance band
Vis	Visible
XRD	X-Ray diffractometer

KAJIAN BAHAN NANOTIUB DAN NANOZARAH TITANIUM DIOKSIDA UNTUK APLIKASI PENGESANAN FOTO ULTRA-LEMBAYUNG

ABSTRAK

Bahan nanostruktur TiO_2 (NsM), i.e., nanotiub dan nanozarah telah menarik banyak perhatian berbanding dengan bahan pukalnya kerana mempunyai sintesis yang murah, teknik penyediaan sederhana, kemampuan aplikasi berskala besar, dan pilihan substrat yang luas. Walaupun begitu, kurang penekanan diberikan pada kajian kesan rawatan penyepuhlindapan yang berbeza pada nanotiub TiO_2, terutamanya kesan pelindapkejutan menggunakan cecair nitrogen (N_2). Dalam beberapa tahun kebelakangan ini, kaedah sol-gel telah menjadi salah satu kaedah sintesis yang paling kerap digunakan untuk nanozarah TiO_2 (TNPs). Walau bagaimanapun, kaedah sol-gel berdasarkan kompleks laluan sitrat telah membebaskan produk sampingan gas yang boleh memudaratkan kesihatan. Selain daripada itu, sintesis TNPs yang halus untuk aplikasi pengesanan foto ultra-lembayung tetap menjadi cabaran. Untuk mengatasi masalah ini, kajian ini bertujuan untuk mengkaji kesan rawatan penyepuhlindapan yang berbeza dan kaedah sol-gel yang diubahsuai pada sifat dan prestasi pengesanan foto ultra-lembayung TNTs dan TNPs, masing-masing. Kajian ini dibahagikan kepada dua bahagian. Bahagian pertama tertumpu pada pertumbuhan TNTs melalui anodisasi elektrokimia dan prestasi pengesanan foto ultra-lembayung TNTs. Analisis pembelauan sinar-X (XRD) menunjukkan bahawa TNTs yang disepuhlindap dan dilindapkejut menggunakan cecair N_2 menunjukkan perbezaan yang ketara dalam peralihan fasa dan dominasi pesawat berbanding dengan TNTs yang dilindapkejut dalam udara ambien. Ia juga mendedahkan bahawa pelindapkejutan cecair N_2 dapat menekan peralihan fasa anatase menjadi rutil di mana TNTs yang dilindapkejut dengan

menggunakan cecair N_2 mempunyai kandungan anatase yang lebih tinggi dibandingkan dengan TNTs yang dilindapkejut dalam udara ambien, terutamanya pada 750°C. Walaupun mempunyai parameter anodisasi yang sama, keadaan penyepuhlindapan dan pelindapkejutan yang berbeza juga mengubah TNTs dari segi ukuran pori dan ketebalan dinding. TNTs yang disepuhlindap pada 650°C dengan kehadiran wap dan dilindapkejutkan dengan menggunakan cecair N_2, menunjukkan prestasi pengesanan foto ultra-lembayung yang memberangsangkan dari segi kepekaan (~16084 % pada 0.5 V), responsiviti (~1764.2 mA / W pada 2 V), masa kenaikan (6-7 s) and pemulihan (7-9 s). Bahagian kedua kajian difokuskan pada pertumbuhan TNPs melalui kaedah sol-gel dan prestasi pengesanan foto ultra-lembayung TNPs. Kajian menunjukkan bahawa TNPs (anatase) yang berasal dari kaedah sol-gel menunjukkan pengurangan ukuran zarah sebanyak ~60% daripada TiO_2 komersial selepas rawatan haba. Dalam kajian ini, pengesan photo ultra-lembayung difabrikasi dengan menggunakan papan Flame Retardant 4 (FR-4) sebagai substrat. Hasil kajian menunjukkan bahawa pengesan foto menampilkan kepekaan (~2764 %) dan responsiviti (~66.14 mA / W) yang tinggi pada pincang 5 V di bawah pencahayaan UV-A.

STUDY OF TITANIUM DIOXIDE NANOTUBES AND NANOPARTICLES FOR ULTRAVIOLET PHOTODETECTION APPLICATION

ABSTRACT

TiO_2 nanostructured material (NsM), i.e., nanotubes and nanoparticles, have attracted a great deal of attention compared to its bulk materials due to their inexpensive synthesis, simple preparation techniques, and the wide choice of substrate options. Despite this, less emphasis was given to the study of different annealing treatment effects on TiO_2 nanotubes (TNTs), particularly the effect of quenching using liquid nitrogen (N_2). In recent years, sol-gel method has been one of the most frequently adopted synthesis methods for TiO_2 nanoparticles (TNPs). However, sol-gel method based on citrate-route complex has raised some health concerns due to its liberation of health-threatening gaseous by-products. Apart from that, synthesis of fine TNPs for photodetection domain remains a challenge. To overcome these issues, present work was intended to study the effect of the different annealing treatment and modified sol-gel method on the properties and the photodetection performance of TNTs and TNPs, respectively. The study was divided into two parts. The first part focused on the growth of TNTs via electrochemical anodization and their UV photodetection performance. X-ray diffraction (XRD) analysis showed that TNTs annealed and quenched using liquid N_2 exhibited significant dissimilarities in the phase transition and plane dominance compared to that of air quenched. It also revealed that the liquid N_2 quenching could suppress anatase's phase transition into rutile whereby TNTs quenched using liquid N_2 had higher anatase content than those air quenched, particularly at 750°C. Varied annealing quenching conditions also modified the pore size and wall thickness of TNTs. The remarkable UV photodetection

performance was credited to TNTs annealed at 650°C in the presence of water vapour and quenched using liquid N_2, with sensitivity ~16084 % (biased at 0.5 V), responsivity ~1764.2 mA/W (biased at 2 V), and ideal rise (6-7 s) and fall time (7-9 s). The second part of the study was focused on the growth of TNPs via sol-gel route and their UV photodetection performance. The study revealed that the sol-gel derived TNPs (anatase) exhibited notable particle size reduction up to ~60 % of commercial TiO_2 after heat treatment. In this work, the UV photodetector was fabricated on a patterned Flame Retardant 4 (FR-4) board. The findings indicated that the photodetector exhibited remarkable sensitivity (~2764 %) and responsivity (~66.14 mA/W) at 5 V bias under UV-A illumination.

CHAPTER 1

INTRODUCTION

1.1 Overview

Nanostructured material (NsM) is low dimensional material with the characteristic length scale of 1-100 nanometres in at least one direction [1]. NsM has a high surface-to-volume-ratio, which offers considerably more active surface sites for higher reaction activities [2]. The physical, chemical, electrical, and optical properties of NsM are distinctly different from their bulk counterparts [1, 3], owing to the change in the dimensionality of the system and atomic structure. The advancement in technology has made the synthesis of material at nanoscale with controlled zero-, one- and two-dimensionality become possible. The synthesis of materials at nanoscale has brought about the drastic change in the electronic density of states and the band structure of the material. Figure 1.1 shows the way semiconductors' electronic density changes with different degrees of reduced dimensionality.

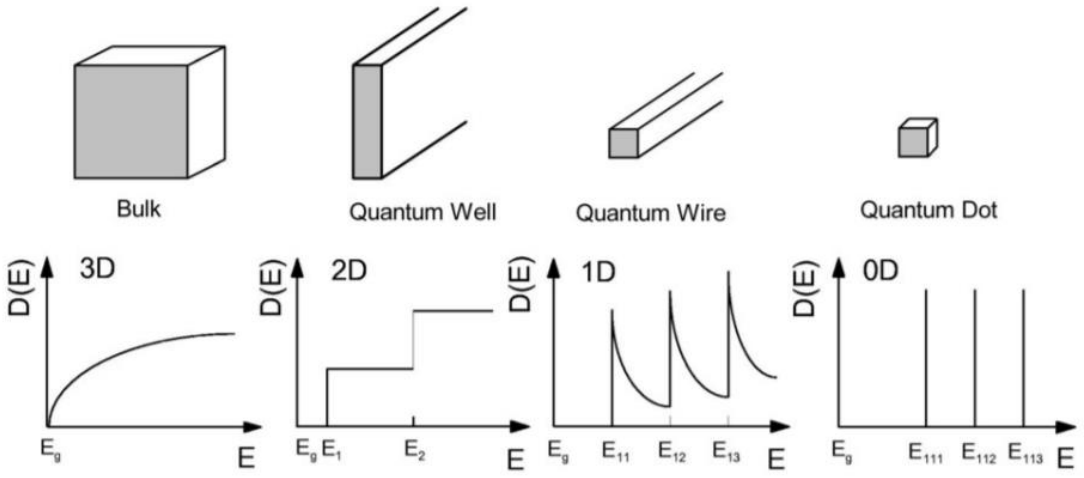

Figure 1.1 The changes in the density of states (DOS) for quantum confined structures [4].

Zero-dimensional (0D) NsM has all dimensions measured within nanoscale, and the most representative of 0D is nanoparticles (NPs). The NPs may exist in various

shapes and forms. One-dimensional (1D) NsM has one dimension outside the nanoscale, resulting in needle-like nanomaterial. 1D NsM can be categorized into two major forms, *i.e.,* nanorods/nanowires and nanotubes. Both 0D and 1D NsM can be amorphous or crystalline, depending on the annealing treatment provided. They also can be crystalline or polycrystalline, which exist individually or incorporated in a matrix.

Titanium dioxide, TiO_2, is one of the metal oxides that has recently gained increasing scientific interest, benefiting from its high chemical stability, excellent photoelectrochemical, optical, and electronic properties [5]. Various methods have been extensively utilized to synthesize TiO_2 NsM, such as electrochemical anodization, sol-gel, and hydrothermal methods. Due to its inexpensiveness, chemical stability, and non-toxicity, absence of absorption in the visible light region as well as high photocatalytic activity, it has been widely studied by researchers and utilized as dye-sensitized solar cells [6], gas sensor [7] as well as UV sensor [8].

There have been numerous studies conducted on the Ultraviolet (UV) photodetector based on semiconductor materials, i.e., SnO, ZnO, ZnMgO, Ga_2O_3, TiO_2, NiO, etc [9]. Among these semiconductor materials, UV photodetector based on TiO_2 has been intensively studied, owing to its superior chemical durability, thermal stability, and compact size [10]. The distinctive UV absorption characteristics of TiO_2 make it a feasible candidate in UV photodetection domains. In this project, UV photodetector synthesized from TiO_2 NsM (nanoparticles and nanotubes) will be studied. For that purpose, a detailed study of different annealing and quenching methods on the elemental, morphological, structural, and optical properties of TiO_2 have been conducted. Aside from that, the use of different substrate materials is also

one of the topics included in this work. The relation between those properties and the photodetection of TiO_2 has been extensively studied and discussed as well.

1.2 Problem Statement

Anodic self-organized 1D TiO_2 nanotubes (TNTs) with large specific surface area and well-defined charge carriers transport channels have increased their scientific interest recently. Owing to these features, numerous annealing treatments have been widely conducted to study morphology and the crystal structure of TNTs. However, the effects of different annealing and quenching conditions on TNTs are scarcely discussed. Particularly, the effect of liquid N_2 quenching on the properties of TNTs is also understudied. Therefore, in this work, we have presented an attempt to study the effect of different annealing and quenching treatments on the properties of TNTs, as well as their correlation with the UV photodetection performance.

Aside from that, synthesizing fine TiO_2 nanoparticles (TNPs) for UV sensing remains a challenge. It has been reported that the particle size of the sensing material plays a vital role, particularly in UV sensing [11]. Sol-gel is one of the most promising approaches to produce fine, spherical and uniform-sized metal oxide powders at low processing temperatures [12, 13]. One common route for sol-gel synthesis of TNPs is the citrate-complex route, which requires concentrated citric acid and ammonia [14]. However, due to the compounds used, health-threatening gaseous by-products could be liberated. To overcome these drawback, a simpler and cleaner approach, i.e., hydrolysis of alkoxide precursors using isopropyl alcohol (IPA) and water was adopted to obtain fine metal oxide and ensure that very little to non-carbon-based residues was formed after the calcination.

1.3 Research Objectives

The main objectives of this study are:

i. To study the effect of the different annealing and quenching conditions on the elemental, morphological, structural, optical, and electrical properties of TNTs, as well as their UV photodetection performance.

ii. To investigate the effect of modified sol-gel method on the structural, morphological, and electrical properties of TNPs based UV photodetector on FR-4 substrate.

1.4 Novelties of Research

The novelties of this research lie on the following aspects:

i. The annealed TNTs are quenched using liquid nitrogen for the first time. The outcomes were evaluated and compared with those quenched in ambient air.

ii. TNPs were prepared using modified sol-gel method. Particularly, IPA was used as the hydrolysis agent in sol-gel method instead of the conventional one, i.e., ethanol and citric acid. Apart from that, polyvinyl alcohol (PVA) was also used as the binder for the TNPs.

iii. FR-4 was used as the substrate material for the first time for TiO_2 UV photodetector. The FR-4 was plated with a layer of nickel (Ni) on copper (Cu) followed by gold (Au) to form the electrode patterns.

CHAPTER 2

LITERATURE REVIEW

2.1 Introduction

This chapter provides an overview of the TiO_2 NsM and UV photodetector. The fundamental properties of TiO_2, as well as the synthesis and formation mechanism of TiO_2 nanotube layers, are presented. The importance of annealing treatment and quenching process are reviewed as well. Aside from that, the synthesis method of TNPs is also one of the reviewed topics in this chapter. Finally, this chapter also gives an overview on the platform of the photodetector as well as the research background of the photodetector based on TNTs and TNPs.

2.2 Fundamental Properties of TiO_2

TiO_2 or titania is known for its abundance, non-toxicity, and chemically stability. It has also drawn an extensive scientific interest, owing to its excellent photochemical, optical, and electronic properties. It exists naturally in three crystalline polymorphs, namely rutile, anatase, and brookite [15]. Anatase and brookite phases are metastable, while the most stable crystal form is rutile phase [16]. TiO_2 is also a wide band gap n-type semiconductor with high refractive index. The band gap of TiO_2 is 3.02 eV and 3.23 eV for rutile and anatase, respectively. The electron-hole pair will only be generated when incident photons with wavelength shorter than 380 nm irradiate TiO_2 [17, 18].

Different crystalline phases give rise to different physical properties, and the fundamental properties of anatase, rutile, and brookite are presented in Table 2.1. Crystallization of amorphous TiO_2 into anatase phase take place at 400°C and formation of rutile phase is achieved at 700°C and higher [19]. In fact, the transition of anatase

into rutile is reconstructive, involving the breaking and reformation of bonds [20]. The reconstructive nature of transformation necessitates a contraction of the c-axis and an overall volume contraction of 8 % [21]. This volume contraction justifies the density of rutile which is higher compared to that of anatase. Furthermore, the c-axis of anatase was also found to be significantly longer than that of rutile, owing to more atoms per unit cell of anatase relative to rutile.

Table 2.1 The fundamental properties of anatase, rutile, and brookite.

Properties	Anatase	Rutile	Brookite	Ref.
Molecular weight (g/mol)	79.88	79.88	79.88	[22]
Crystal structure	Tetragonal	Tetragonal	Orthorhombic	[23]
Lattice parameter (Å)	a = 3.785 c = 9.514	a = 4.594 c = 2.959	a = 9.184 b = 5.447	[24, 25]
Atoms per unit cell (Z)	4	2	8	[24, 25]
Unit cell volume ($Å^3$)	136.25	62.07	257.38	[24, 25]
Density (g/cm^3)	3.79	4.13	3.99	[24, 25]
Band gap (eV)	3.23	3.02	3.20	[26-28]
Melting point	Transform to rutile	1830-1850 °C	Transform to rutile	[29]
Hardness (Mohs)	5.5-6.0	6.0-6.5	5.5-6.0	[29]
Specific gravity	4.0	4.2	4.0	[30]
Refractive index	2.488-2.561	2.605-2.616	2.583-2.700	[30]

The geometrical structures of the unit cells of anatase and rutile TiO_2 and their respective polymorph were shown in Figure 2.1, with grey and red spheres representing Ti^{4+} and O^{2-}, respectively. The experimentally reported tetragonal (I4/amd) and tetragonal ($P4_2/mnm$) structures for anatase and rutile TiO_2 were adopted as initial structures [31]. The unit cells of anatase TiO_2 consist of four Ti atoms and eight O atoms, whereas that of rutile TiO_2 consist of two Ti atoms and four O atoms. Apart from that, both crystal structures also contain TiO_6 octahedra sharing four edges in anatase and two in rutile, as shown in Figure 2.1 (b).

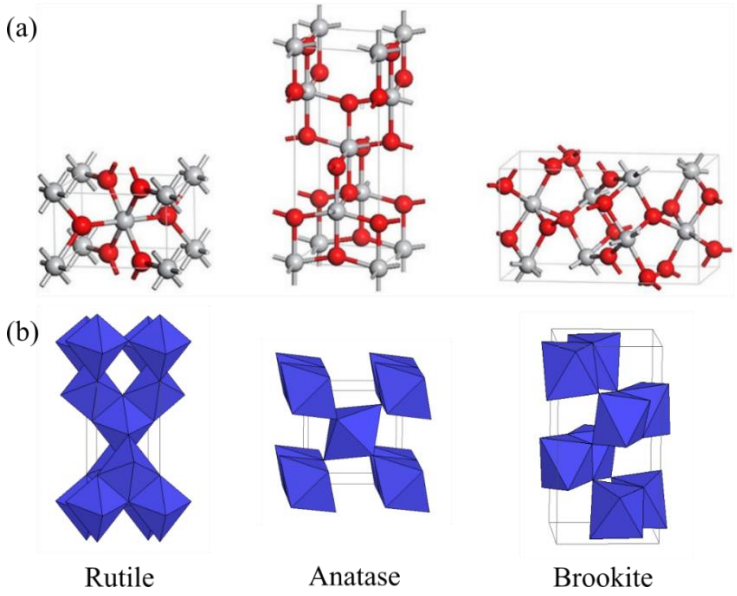

Figure 2.1 (a) Unit cell and (b) three-dimensional representation of the arrangement of TiO_6 octahedra of TiO_2 rutile, anatase, and brookite [32].

2.3 Synthesis of Self-organized TiO_2 Nanotubes Layers

2.3.1 Electrochemical Anodization

Various synthetic strategies have been discovered to grow 1D NsM, such as TNTs. The commonly used techniques include electrochemical anodization method [33, 34], sol-gel method [35, 36], and hydrothermal method [37, 38]. Electrochemical anodization is one of the most promising methods favoured by the researchers to fabricate spatially periodically ordered nanostructures consisting of highly ordered TNTs arrays. Electrochemically anodized TNTs are featured by smooth surface and regularly aligned nano-architectures are grown perpendicularly from the foil, providing a beneficial medium for efficient charge separation and transfer [39]. More intriguingly, the anodized TNTs have shortened carrier diffusion length compared to that of bulk counterparts, which considerably minimizes the energy loss caused by the electron transition among nanoparticles (NPs). Furthermore, electrochemical anodization also allowed the precise control of nanotubes dimensions and simple setup and fabrication

processes. Due to the numerous advantages offered, electrochemical anodization was utilized to grow the TNTs from Ti foil.

Electrochemical anodization is an electrolytic passivation process where oxide layer grows on certain metals. Usually, a thin yet dense barrier oxide of uniform thickness is capable of growing on metals under specific conditions. Parameters such as electrolyte, temperature, applied voltage, anodization duration, etc., were known as important factors to affect the nanostructures' growth [40, 41]. As illustrated in Figure 2.2, electrochemical anodization is conducted in a two-electrodes electrochemical cell whereby metal (in this case, Ti foil) be treated as working electrode (anode) and connected to positive terminal of power supply while platinum foil functions as counter electrode (cathode) and connected to negative terminal of power supply. Typically, both anode and cathode are partially immersed in an electrolyte bath.

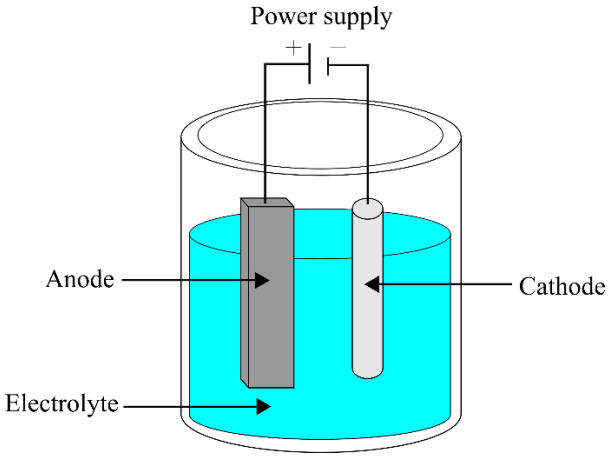

Figure 2.2 Schematic diagram of the electrochemical cell setup.

2.3.2 Formation Mechanism of TiO_2 Nanotubes

The formation of TNTs is determined by two competitive reactions: (i) oxide formation at the oxide/metal interface by oxygen anions (O^{2-} and OH^-), and the dissolution reaction initiated by F^- in the electrolyte. The detailed description regarding of formation mechanism is as below:

a) In oxide formation, the electrolysis of water results in the formation of O^{2-} or OH^- anions on the electrolyte/oxide interface. The anions diffuse via the oxide layer toward the metal interface to react with Ti^{4+} coming from the opposite direction, resulting in the generation of a thin layer of amorphous TiO_2 on Ti substrate. When sufficient high external potential is applied, the weak Ti-O bonds can be easily broken, resulting in the dissolution of the initially formed amorphous TiO_2 to produce Ti^{4+}. The formation is described using the equations below [42-46]:

Anode: $Ti \rightarrow Ti^{4+} + 4\ e^-$ (2.1)

$Ti^{4+} + 4\ OH^- \rightarrow Ti\ (OH)_4$ (2.2)

$Ti^{4+} + 2\ O^{2-} \rightarrow TiO_2$ (2.3)

$Ti\ (OH)_4 \rightarrow TiO_2 + 2\ H_2O$ (2.4)

Cathode: $4\ H^+ + 4\ e^- \rightarrow 2\ H_2$ (2.5)

Overall: $Ti + 2\ H_2O \rightarrow TiO_2 + 4\ H^+ + 4\ e^-$ (2.6)

b) As for the dissolution reaction, the electric field generated by the supply of potential causes the amorphous TiO_2 to react with F- at electrolyte/ oxide interface to produce $[TiF_6]^{2-}$ complex. The $[TiF_6]^{2-}$ formed dissolves the TiO_2 layer and resulting in the formation of random tiny pits and cracks on the TiO_2 layer.

$TiO_2 + 6\ F^- + 4\ H^+ \rightarrow TiF_6^{2-} + 2\ H_2O$ (2.7)

c) As the time passes by, these tiny pits will grow larger and finally become pores, which further evolved into TNTs.

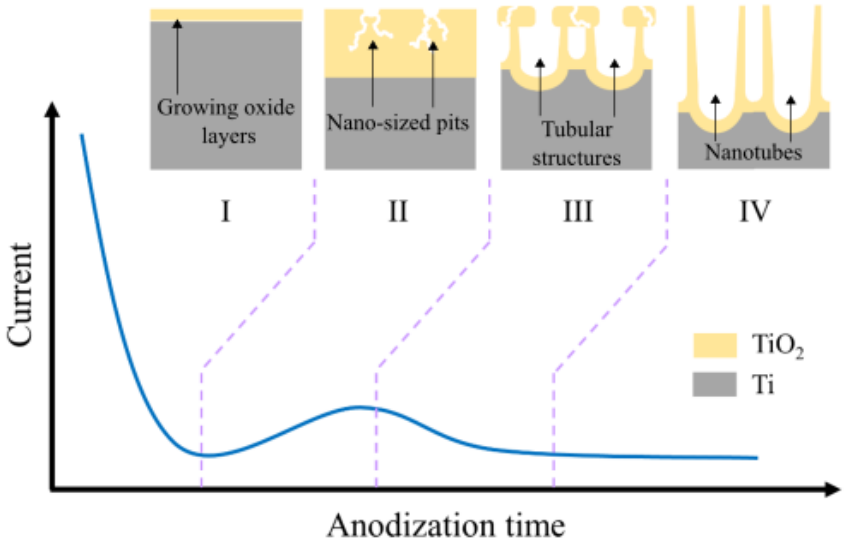

Figure 2.3 The current-time curve for the formation of TiO_2 nanotubes [47].

As shown in Figure 2.3, the current-time (I-t) behaviour obtained from the potentiostatic preparation of TNTs explains the overall mechanism. Initially, a drastic drop in current is evident with the increasing resistance of the rapidly growing oxide layer (I). Then, the current starts to increase gradually, signifying the formation of nano-sized pits by the attack of F^- ions (II). The pits formed provide a strengthening spot for the electric field created, thereby attracting more anions to take part in the oxide formation and dissolution reactions. The continual growth of tubular structures beneath the pits results in the reduction of current (III). When oxide formation and dissolution reach an equilibrium, the current converges (IV).

2.3.2(a) Structural and Geometrical Influence

The geometry of TNTs, i.e., tubular pore diameter, thickness, and length, was reported to be strongly influenced by the anodization parameters such as anodization potential, anodization duration, and the composition of the electrolytes. The detailed discussions on each of the parameters are as below:

i. Anodization Potential

The pore diameter and thickness of TNTs are significantly influenced by the anodization potential applied [48]. At low potential, TNTs with few hundreds of nanometer in length and a few tens of nanometer in diameter were reportedly formed. When the applied potential is significantly low, the electric field dissolution rate surpasses that of electrochemical etching rate, reducing the barrier oxide layer's thickness and favouring the pores formation instead of nanotubes. On the contrary, when the applied potential is too high, the rate of electrochemical etching will become higher than that of electric field dissolution, speeding up the increase of the barrier layer's thickness, which would retard the growth of pores into nanotubes, as well. The diameter of TNTs was found to be increased with the applied voltage in the range of 20-60 V [49]. The trend could be ascribed to the extent of electric field dissolution itself. At the early stage of anodization with lower potential applied, less electric field dissolution limits the formation of pits. However, when the applied potential is increased, more pits are being formed, which would be subsequently etched to form larger pores under high electric field dissolution [50]. Consequently, higher anodization voltage leads to the formation of TNTs with larger diameters.

ii. Anodization Duration

The anodization duration influences the TNTs formation significantly, whereby there's no TNTs if the anodization time is too short [51]. It was reported that the minimum time required to form TNTs is 15 minutes, with increasing time resulted in the formation of highly ordered TNTs. Similarly, it was also found that nanoporous structures and visibly clear nanotubular structures could only be formed after 5 minutes and 10-20 minutes of anodization, respectively [40].

Apart from that, short and narrow TNTs would be formed easily also at the anodization time of 5 minutes [52].

iii. Electrolytes

Electrolyte plays a vital role in the formation of TNTs as the electric field dissolution rate is influenced by the composition of electrolyte (fluoride ions), whereby increasing fluoride ions concentration will increase the electric field dissolution rate. Therefore, only specific fluoride ions concentration range favour the formation of TNTs. Furthermore, it was reported that longer TNTs could be formed using fluoride-containing electrolytes instead of HF-containing buffer electrolytes species of highly viscous (organic) electrolytes [53]. To date, two types of electrolytes were generally used to synthesize TNTs, namely organic and aqueous electrolytes. The organic electrolytes such as $(NH_4)H_2PO_4/NH_4F$ [54] and $(NH_4)_2SO_4/NH_4F$ [55] was found to form TNTs of longer length and better self-organized. As for aqueous electrolytes, by having higher diffusibility and concentration of ions, there is higher current density than that of organic electrolytes [56]. The anodic condition could be better controlled in the viscous (organic) electrolytes, creating two different environments along the TNTs. One is inert at the top, while another is chemically reactive at the bottom. Subsequently, the oxide dissolution at the top of TNTs is inhibited, making the formation of long TNTs possible [57].

2.4 Synthesis of TiO_2 Nanoparticles

2.4.1 Sol-gel Method

TNPs could be prepared by various methods, such as sol-gel [35, 36], electrodeposition [58] and hydrothermal [37]. Among these methods, sol-gel has been known as one of the most promising approaches for preparing nano-sized metal oxide

materials and has been widely utilized to prepare TNPs. The sol-gel process is a method commonly used to synthesize solid materials from small molecules via the conversion of small molecules (precursors) into a colloidal solution (sol) and then into an integrated network (gel) consisting of either discrete particles or network polymers.

The numerous advantages offered by the sol-gel method have aroused great scientific interest and has been widely used in the preparation of metal oxides nanoparticles (MONPs). Sol-gel technique is known for its inexpensiveness and budget-friendly process to prepare metal oxides and the ability to have control over the doping process or addition of transition materials. It is also controllable to obtain the required oxide features with a high degree of homogeneity and purity. Besides, it also produces fine, spherical powders of uniform size and allows the use of low processing temperatures (<100°C) and molecular level composition homogeneity [59].

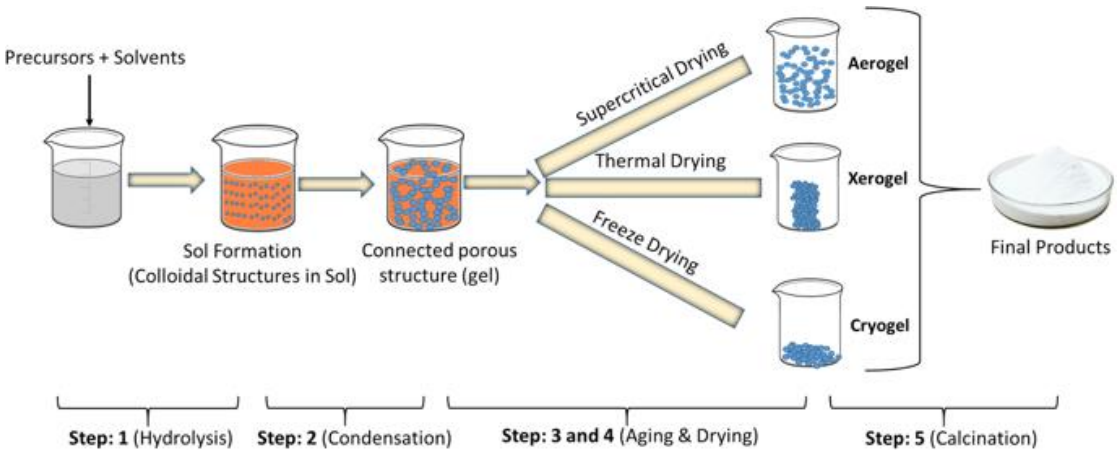

Figure 2.4 The steps involved in the sol-gel method to synthesize nanoparticles [60].

As shown in Figure 2.4, the sol-gel process comprises five steps: (1) hydrolysis, (2) condensation/polymerization of monomers, (3) aging, (4) drying and (5) calcination. These processes are influenced by several experimental parameters such

as pH, temperature, concentration of the reactants, and presence of additives. The detailed descriptions of each stage are as below:

i. Step 1

Hydrolysis of the precursors, for example, metal alkoxides, occurs in water or alcohols, as shown in Figure 2.4. In this process, water or organic solvents (i.e., alcohols) provide oxygen, which is critical for forming metal oxide. If the reaction medium used is water, it is known as an aqueous sol-gel method. On the contrary, it is a non-aqueous sol-gel method if organic solvent is used as a reaction medium. The general chemical reaction for the hydrolysis process is given below:

$$\text{M-OR} + H_2O \rightarrow \text{MOH} + \text{ROH (Hydrolysis)} \quad (2.8)$$

where M=metal, R=alkyl group (C_nH_{2n+1}). The gel formation is strongly affected by the amount of water, whereby a higher water content enables the formation of a higher proportion of bridging to nonbridging oxygens, resulting in formation of more polymerized and more branched structure during the condensation [61].

ii. Step 2

In this step, condensation of adjacent molecules occurs via elimination of water/alcohol, leading to formation of metal oxide linkages. Then, the polymeric networks grow to colloidal dimensions in the liquid state. Condensation is comprised of two processes, namely olation and oxolation [60]. Olation is a formation of hydroxyl (-OH-) bridge between two metal centres (metal-hydroxy-metal bonds), whereas in oxolation an oxo (-O-) bridge is formed between two metal centres (metal-oxometal bonds). The general chemical reaction for the condensation process is given below:

$$M\text{-}OH + XO\text{-}M \rightarrow M\text{-}O\text{-}M + XOH \text{ (Condensation)} \quad (2.9)$$

Where M=metal, X=H or alkyl Group (C_nH_{2n+1}). Consequently, condensation increases the viscosity of solvent, causing the formation of a porous structure maintaining liquid phase called gel. In this context, the alkoxide and pH of the solution determine the size and the cross-linking within the colloidal particles [62-64].

iii. Step 3

In aging process, continual changes of the structure and properties of the gel take place. Meanwhile, polycondensation also occurs within the localized solution, along with the reprecipitation of the gel network, which ultimately leads to reduction in porosity and increase of thickness between colloidal particles [60].

iv. Step 4

There are different drying processes, namely supercritical drying, atmospheric/thermal drying and freeze-drying. Each of the processes influences the structure of the gel network differently. Supercritical drying is used to obtain aerogels with high pore volume and surface area without affecting the original gel network [60]. On the contrary, thermal drying is the process in which the porous gel is heated at high temperature to cause the densification [65] and the removal of the pores from gel, resulting in the formation xerogel, which features a relatively low surface area and pore volume and high shrinkage of the gel [66]. As for freeze drying, the solvents are frozen to form cryogel, which has low gel network shrinkage compared to that of xerogel.

v. Step 5

In the last step, the gel formed earlier is subjected to thermal treatment/calcination to eliminate the residues and water molecules. The calcination temperature is a critical parameter to control the pore size and the density of the material [60].

2.5 Heat Treatment of TiO_2

Heat treatment plays a vital role in synthesising the particles, changing morphology, crystallinity, and porosity. It can also reduce the surface area, lose hydroxyl group, and, most importantly, induce phase transformation. In the case of TiO_2, heat treatment helps regulate the crystallinity of TiO_2, whereby amorphous TiO_2 can be transformed into crystalline structures of anatase or rutile phase, depending on the annealing temperature [67]. More importantly, the nanostructure and the crystalline state of TNTs is of considerable significance due to the improvement in optimizing many chemical and physical reactions by developing the anatase or rutile crystalline phase [68, 69]. It has been reported that the formation of anatase phase takes place between 230 and 280°C [21]. Phase transformation of amorphous TiO_2 into the anatase phase was also known to cause the collapse of pores in the TiO_2 powder, resulting in decreased surface area with calcination time and the heating rate [70]. In particular, slow heating rates offer relatively mild conditions for phase transformation [71]. Furthermore, the transition of anatase into rutile phase has been reported to occur between 500 and 600°C [72]. However, there is no distinct transition temperature of anatase and rutile, and it usually occurs at a wide range of temperatures (400-1000°C) [21, 73]. In fact, the phase conversion is time-dependent, and it is affected by particle size and shape, surface area, volume of the sample, annealing atmosphere, heating rate and the presence of impurities [21]. Table 2.2 summarizes the typical heat treatment's

conditions and durations of TiO_2 that have been reported earlier by other literatures in recent years.

Table 2.2 Typical heat treatment of TiO_2 reported by other literature in recent years.

Heat treatment conditions	Heat treatment duration	The significance of the heat treatment employed	Ref.
Annealed from 300-800°C in air	2 hours	Low temperatures (below 600°C) have no great influence on surface morphology and architecture of the TNTs sample, and the prepared TNTs can be stable up to 600°C.	[74]
Calcined at 300, 400, 500, 600, 700, and 800°C	4 hours	A mixture of brookite and anatase phase was obtained at heat treatment less than 400°C. The rutile phase was formed above 500°C. The mixtures of anatase, rutile and brookite was obtained at temperatures between 500 and 600°C. Anatase and brookite phase transformed completely into rutile phase at 800°C.	[75]
Annealed from 400 to 1000°C in air	2 hours	The anatase-to-rutile transformation occurs between 500 and 600 °C.	[76]
Annealed at 700°C in air	12 hours	The amorphous oxide layer induced by anodization led to the simultaneous anatase and rutile phase growths during the first 30 minutes of annealing.	[77]
Heat treated at 350, 450, 550 and 650°C	N/A	N/A	[78]

2.6 Quenching Process

The increasing demand of the different environments and jobs has required the use of tailored metals feature altered hardness, toughness and strength with intact chemical composition. Thus, heat treatment has become vital in recent days as it can yield tailored metal. Metals can be heat treated via numerous methods, and one of the well-established methods is quenching.

Quenching is a rapid cooling process used to bring a workpiece back to the room or lower temperature to inhibit undesired low-temperature processes from happening by minimizing the window of time in which these undesired reactions are thermodynamically active. Prior to the quenching process, metal heating is usually carried out at a temperature somewhere above the temperature at which the

recrystallization occurs but below its melting temperature [79]. The heating of metal may last for a certain period for the material to reach the desired temperature before it is quenched in a medium to regain its room temperature. The extent of time to which the metal is quenched determines the distribution of coolness from quenching throughout the thickness of the materials. Furthermore, given the capability of reducing the crystal grain size of metallic materials and increasing their hardness, quenching has been extensively utilized to strengthen and harden the steel and cast-iron alloys.

In general, quenching can be conducted in numerous types of quenching media, each with its distinct quenching properties. The quenching speed, quenching media environmental concerns, quenching media replacement, and quenching media cost determines the types of quenching media used. Below shows the main type of quenching media [79]:

a) Air

   Air is a commonly used quenching medium in quenching metals, owing to its availability and profusion on earth. Air quenching can be easily witnessed in daily life as any heated material allowed to cool to room temperature by merely being left alone is known as air quenched. Despite this, there is also intentional air quenching whereby it is compressed and forced around the metal being quenched, facilitating the cooling process compared to that of still air.

b) Oil

   Oil provides a faster cooling rate than compressed air. In quenching using oil, a heated metal is lowered into an oil-filled tank. The application usually determines the type of oil used, considering their varying cooling rates and flashpoints.

c) Water

Water is also one of the quenching media that offers a fast-cooling rate and is comparable or even faster than that of oil. Quenching using water is conducted similarly to that of oil, whereby metal is submerged in a tank filled with water instead of oil. Furthermore, the concern of media's flammability could be avoided if water is used as quenching media.

d) Liquid N_2

Liquid N_2 is N_2 in a liquid state at low temperature (-195.79°C (77 K; -320°F) boiling point at sea level), produced industrially via fractional distillation of liquid air. It is a compact source of dry N_2 gas and can be easily transported, as pressurization is not required. Furthermore, its capability of maintaining temperatures far below the water freezing points makes it extremely useful in a wide range of applications, such as coolant, cryogenics, cryotherapy, etc. [80].

2.7 Photolithography

Photolithography, also known as optical lithography, is applied to microfabricate the pattern parts on a thin film or the bulk of a substrate. It is the process of transferring geometric shapes from a photomask to photosensitive chemical photoresist of the substrate via light. As shown in Figure 2.5, the photolithography process comprises four main steps: substrate cleaning, photoresist deposition, UV exposure, and post-baking [81]. The photoresist can be either positive or negative. In positive photoresists, UV light is used to irradiate the resist and then remove the material underneath it. In these resists, the UV light exposure changes the resist's chemical structure and increase its solubility in the developer. The exposed resist is then washed away by the developer solution, leaving windows of the bare underlying material. As for negative photoresist, UV light exposure polymerize the negative resist, making it

more difficult to dissolve. Therefore, the negative resist remains despite the exposure to the developer and only the unexposed portions are removed.

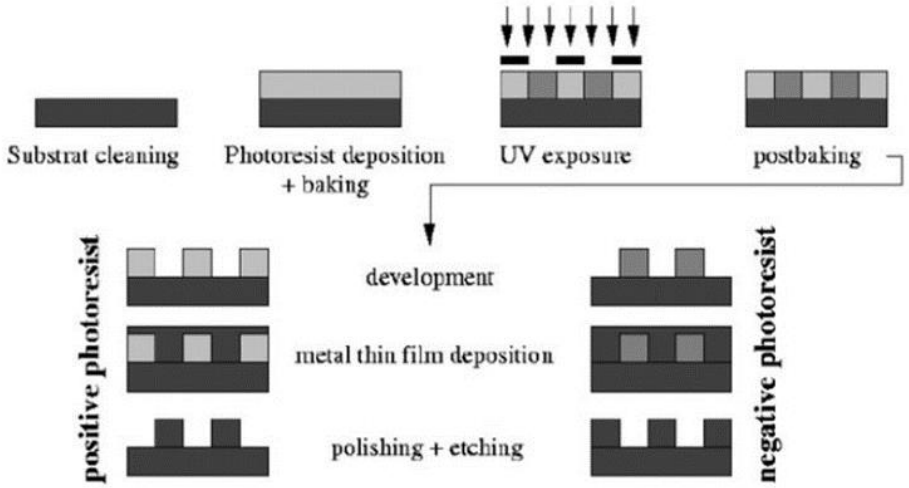

Figure 2.5 The steps involved in photolithography [81].

2.8 Theoretical Concept of Photodetector

The photoelectric effect is the phenomenon in which photons interact with semiconductor materials, resulting in electron-hole pairs' formation. The electrons produced in this way are termed as photoelectrons, and these electrons can be directed to the electrode under the influence of the external electric field [82]. There are two categories of photoelectric effect, namely photoelectric emission and photoconductivity. Photoelectric emission is an external process that occurs when the photogenerated electrons escape from the semiconductors' surface into the vacuum and move as free electrons. On the contrary, photoconductivity is an internal process in which photogenerated electrons remain inside semiconductor instead of escaping into a vacuum, leading to increased photoconductivity. An example of this process is photodetectors.

2.8.1 Working Principle of Photodetector

Photodetectors, also known as photosensors, are detectors of light or other electromagnetic radiation. Main sensing materials are usually made up of semiconductor materials with both ends connected to metals acting as electrodes [83]. The photodetector's working principles are as below:

i. When the semiconductor material is illuminated by incident photons with energy greater or equal to its band gap, the absorbed photons promote electrons from the valance band into excited states in the conduction band, leaving behind the positively charged holes in the valance band and thus forming electron-hole pairs, as shown in Figure 2.6.

ii. As shown in Figure 2.7, under the influence of the external electric field, the electron-hole pairs are separated and collected by the electrodes, resulting in the flow of current in the external circuit.

iii. Any changes in the circuit current are detected and presented in the form of output signal.

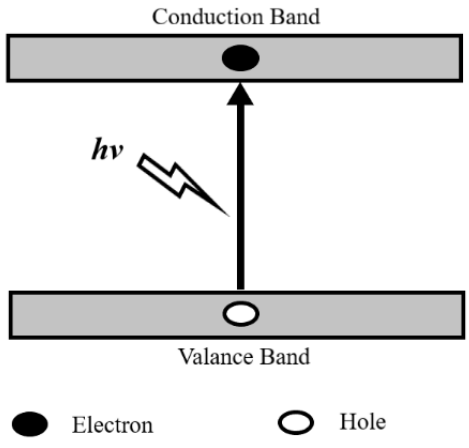

Figure 2.6 The schematic diagram of electron-hole pairs generation.

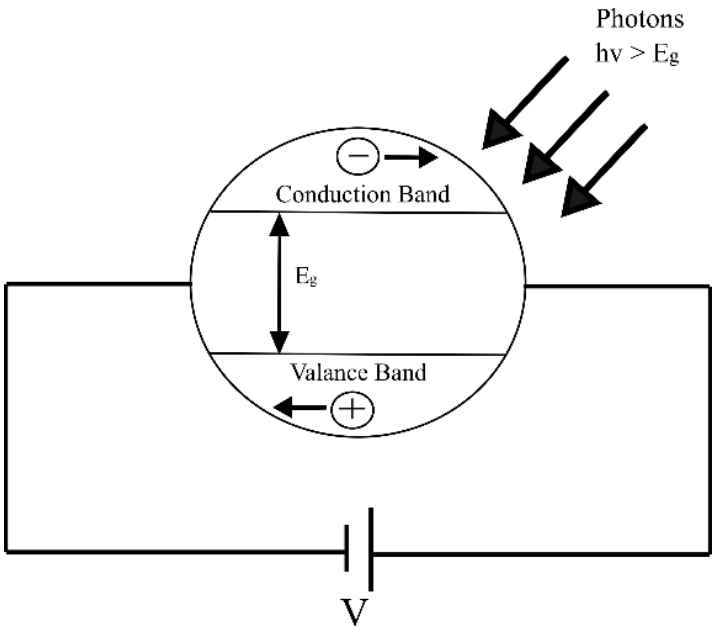

Figure 2.7 Schematic of a typical photodetector.

2.8.2 Photoelectric Characteristics

In evaluating the photodetector's performance, certain parameters need to be investigated, which consist of reproducibility, sensitivity, responsivity, quantum efficiency, photo response speed (rise time and fall time).

2.8.2(a) Sensitivity

The sensitivity (S) is defined as the relative change in the current density upon exposure to UV irradiations [84] and was calculated by using expression Eq. (2.10) [85]:

$$S = \frac{I_{light} - I_{dark}}{I_{dark}} \times 100\% \tag{2.10}$$

where I_{dark} and I_{light} are the dark and photocurrent density, respectively.

2.8.2(b) Responsivity

Responsivity, R is an important parameter which commonly used to measure the efficiency of the photodetector to convert the incident light into current, and it can be defined as the photocurrent of the photodetector generated, $I_{ph}\,(A)$, per optical

intensity (light flux), P (mW/cm^2), on the effective area, A (cm^2) Responsivity can be calculated using the following Eq. (2.11):

$$R = \frac{I_{ph}}{PA} \tag{2.11}$$

2.8.2(c) Quantum Efficiency

The quantum efficiency, η is the ratio of the number of carriers collected by the photodetector to the number of photons of a given energy incident on the photodetector itself. The quantum efficiency may be presented either as a function of wavelength or as energy, which can be calculated by using following Eq. (2.10):

$$\eta = R\frac{hc}{q\lambda} \tag{2.12}$$

Where R (mA/W) is the calculated responsivity at incident wavelength λ (nm), h (eV) is Planck's constant, c (m/s) is the velocity of light and q (c) is the electron charge.

2.8.2(d) Rise Time and Fall Time

Rise time (τ_r) is defined as the time taken for the photocurrent of the photodetector to increase from 10 % to 90 % of its steady states, and otherwise for fall time (τ_f). Rise/fall time has been one of the crucial parameters in the evaluation of photodetector performance. In order to be titled as a good photodetector, one needs to respond rapidly to the incident light. The shorter the rise/fall time, the better is the performance of the photodetector. The rise/fall time of the photodetector was evaluated by enlarging the current over time curve of the photodetector upon illuminated by light pulses, as illustrated in Figure 2.8.

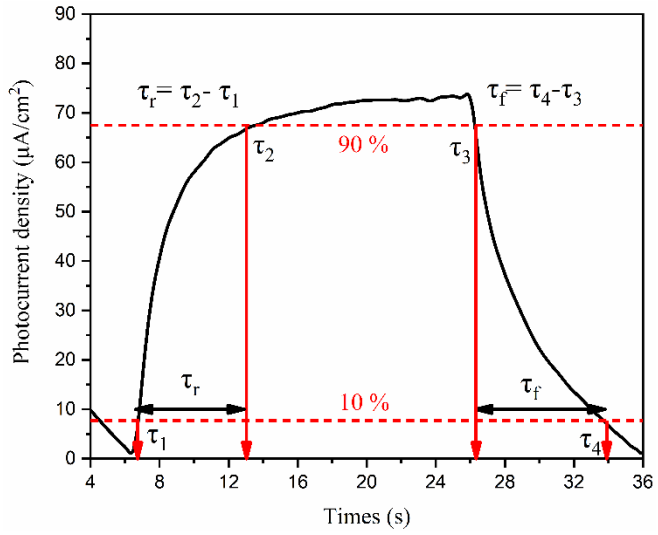

Figure 2.8 Method used to determine the rise/fall time of the photodetector.

2.8.3 Substrate Material for Photodetector

In recent years, numerous approaches have been applied to the study of the substrate material used for UV photodetection, and among the most commonly used material are FTO glass [86], silicon [87] , etc. By having high strength, good corrosion tolerance and excellent biocompatibility, Ti and Ti alloys have been widely used as high-quality light corrosion-resistant structural material and essential biomedical material [88-92]. Pure Ti's allotropic transition temperature is around 882°C, and Ti can form various crystal structures at different temperatures, comparable to other hexagonal closed packed (HCP) metals (such as Zr and Hf). Pure Ti and most Ti alloys form HCP structure called α-Ti under the low-temperature condition, and it is converted into a body centred cubic (BCC) structure under the high-temperature condition, which is called β-Ti [93]. Aside from the substrate mentioned above, printed circuit board (PCB) has gained increasing scientific interest in the fabrication of the sensor. PCB is classified as rugged nonconductive boards constructed on substrate-based structures, typically used to provide electrical connection and mechanical support to a circuit's electrical components [94]. They are common in electronic devices and are in most